molecular pharmaceutics

articles

A Novel Octreotide Modified Lipid Vesicle Improved the Anticancer Efficacy of Doxorubicin in Somatostatin Receptor 2 Positive Tumor Models

Junlin Zhang,† Wu Jin,† Xueqing Wang, Jiancheng Wang, Xuan Zhang, and Qiang Zhang*

State Key Laboratory of Natural and Biomimetic Drugs, School of Pharmaceutical Sciences, Peking University, Beijing, 100191, P. R. China

Received February 1, 2010; Revised Manuscript Received April 27, 2010; Accepted June 4, 2010

Abstract: Octreotide (Oct) is a potential ligand due to its high affinity to somatostatin receptors (SSTRs), especially subtype 2 (SSTR2), as many tumor cells specifically overexpress SSTR2. In this study, we conjugated Oct to the PEG end of DSPE-PEG and prepared a novel doxorubicin (DOX)-loaded and Oct-modified sterically stabilized liposomes (Oct-SSL-DOX), in order to facilitate intracellular delivery of chemotherapeutic agent to the related tumor cells through active targeting and finally improve its antitumor activity. Three cells were proved to be different in expression level of SSTR2 and were used as model or control. It was demonstrated by fluorescence spectrophotometry, confocal laser scanning microscopy and flow cytometry that active sterically stabilized liposomes (SSL) increased intracellular delivery of DOX in SSTR2-positive cells, through a mechanism of receptor-mediated endocytosis. Compared to SSL, Oct modification on SSL exhibited little effect on the physicochemical properties of SSL. However, it reduced the circulation time of loaded-DOX to some extent in rats, increased cytotoxicity in SSTR2-positive tumor cells, enhanced drug accumulation in tumor tissue and improved anticancer efficacy in SSTR2-overexpressing tumor model. The correlation was found among intracellular uptake, cytotoxicity, drug distribution in tumor and pharmacodynamics of Oct-SSL-DOX, but not the pharmacokinetics based on plasma drug concentration. In summary, octreotide-modified SSL might be a promising system for the treatment of SSTR2-overexpressing cancers.

Keywords: Octreotide; somatostatin receptors; sterically stabilized liposomes; doxorubicin; antitumor effect

Introduction

Among various drug delivery systems, liposomes represent an advanced technology to provide a biocompatible carrier and favorable pharmacokinetic properties. The development of PEGylated liposomes, also called sterically stabilized liposomes (SSL), which are characterized by long half-life in plasma compartment, has inaugurated a new era in liposomal drug delivery.[1,2] Several chemotherapeutic agents, including doxorubicin (DOX), have been successfully associated to liposomes or SSL[3,4] which are commercially

* Corresponding author. Mailing address: Peking University, Pharmaceutical Sciences Department, 38 Xueyuan Road, Haidian District, Beijing, 100191, China. E-mail: zqdodo@bjmu.edu.cn. Tel/fax: +86-10-82802791.

† These authors contributed equally to this work.

(1) Chonn, A.; Cullis, P. R. Recent advances in liposome technologies and their applications for systemic gene delivery. *Adv. Drug Delivery Rev.* **1998**, *30*, 73–83.

(2) Minko, T.; Pakunlu, R. I.; Wang, Y.; Khandare, J. J.; Saad, M. New generation of liposomal drugs for cancer. *Anti-Cancer Agents Med. Chem.* **2006**, *6*, 537–552.

(3) Xiong, X. B.; et al. Enhanced intracellular delivery and improved antitumor efficacy of doxorubicin by sterically stabilized liposomes modified with a synthetic RGD mimetic. *J. Controlled Release* **2005**, *107* (2), 262–275.

(4) Murphy, E. A.; et al. Nanoparticle-mediated drug delivery to tumor vasculature suppresses metastasis. *Proc. Natl. Acad. Sci. U.S.A.* **2008**, *105* (27), 9343–9348.

10.1021/mp1000235
Published on Web 06/04/2010

available now. DOX, an anthracycline analogue, is one of the most frequently prescribed antineoplastic agents for cancer chemotherapy. However, its cardiotoxicity, which could lead to congestive heart failure or death, compromises its clinical application. DOX encapsulated in PEGylated liposomes, known as Doxil, has reduced cardiotoxicity compared to free DOX.[5,6]

As we know, PEGylated liposomes could significantly improve drug (e.g., DOX) distribution *in vivo*.[7,8] But previous reports, including ours,[3] demonstrated that drug-loaded PEGylated liposomes were very similar to free drug in terms of therapeutic effect. It was quite possible that PEGylated liposomes could only increase drug concentration in tumor tissue, but not the intracellular drug level. On the contrary, it was found that the increased intracellular drug concentration usually led to improved antitumor efficacy. Therefore, the significance of enhancing drug delivery into tumor cells caught the attention of scientists. In fact, various efforts have been made, for instance, modifying PEGylated liposomes with monoclonal antibodies or unique ligands.[9,10] Main ligands reported included folate,[11−13] transferrin,[14] EGF,[15,16] albumin[17] and so on.

Somatostatin (SST) is a neuropeptide that demonstrates a powerful inhibitory action against several endocrine systems, including brain, pituitary, gut, exocrine and endocrine pancreas, adrenals, thyroid, and kidneys. The biological effects of SST are mediated through high-affinity plasma membrane receptors, named SSTRs, which have been demonstrated on a variety of human tumors by classical biochemical binding techniques. Extremely high levels of SSTR expression are generally detected in neuroendocrine tumors,[18] including pituitary adenomas, endocrine pancreatic tumors, gastrointestinal and lung carcinoids, paragangliomas, pheochromocytomas, small cell carcinomas, Merkel cell carcinomas, neuroblastomas and medullary thyroid carcinomas, with a preferential expression of SSTR subtypes 2, 3 and 5.[19]

The value of SST as ligand in targeting delivery systems has been already demonstrated by the clinical use of [111]In-DTPA-octreotide (OctreoScan, Pentetreotide), a radiodiagnostic agent with high binding affinity to SSTRs, especially subtype 2. Pentetreotide was approved for clinical use by the FDA in scintigraphically identifying various neuroendocrine tumors.[20] In addition, somatostatin analogues conjugated with antitumor agents, such as DOX,[21−23] paclitaxel[24,25] and camptothecin,[26,27] have also been assessed and proved potentially in anticancer drug delivery. All commentaries focused on SST and its analogues in tumor diagnosis and therapy convinced us to consider Oct as a potential candidate in ligand−receptor mediated targeting DDS.

It is supposed that coupling Oct to PEGylated liposomes might be favorable for enhancing their binding to SSTR

(5) O'Brien, M. E. R.; et al. Reduced cardiotoxicity and comparable efficacy in a phase III trial of pegylated liposomal doxorubicin HCl (CAELYX™/Doxil®) versus conventional doxorubicin for first-line treatment of metastatic breast cancer. *Ann. Oncol.* **2004**, *15* (3), 440–449.

(6) Harris, L.; et al. Liposome-Encapsulated Doxorubicin Compared with Conventional Doxorubicin in a Randomized Multicenter Trial as First-Line Therapy of Metastatic Breast Carcinoma. *Cancer* **2002**, *94* (1), 25–36.

(7) Uster, P. S.; Working, P. K.; Vaage, J. Pegylated liposomal doxorubicin (DOXIL®, CAELYX®) distribution in tumour models observed with confocal laser scanning microscopy. *Int. J. Pharm.* **1998**, *162* (1−2), 77–86.

(8) Vail, D. M.; et al. Pegylated liposomal doxorubicin: Proof of principle using preclinical animal models and pharmacokinetic studies. *Semin. Oncol.* **2004**, *31* (Suppl. 13), 16–35.

(9) Forssena, E.; Willisb, M. Ligand-targeted liposomes. *Adv. Drug Delivery Rev.* **1998**, *29*, 249–271.

(10) Eliaz, R. E.; Francis, C.; Szoka, J. Liposome-encapsulated Doxorubicin Targeted to CD44: A Strategy to Kill CD44-overexpressing Tumor Cells. *Cancer Res.* **2001**, *61*, 2592–2601.

(11) Lu, Y.; et al. Role of Formulation Composition in Folate Receptor-Targeted Liposomal Doxorubicin Delivery to Acute Myelogenous Leukemia Cells. *Mol. Pharmaceutics* **2007**, *4* (5), 707–712.

(12) Gabizon, A.; et al. In Vivo Fate of Folate-Targeted Polyethylene-Glycol Liposomes in Tumor-Bearing Mice. *Clin. Cancer Res.* **2003**, *9*, 6551–6559.

(13) Leamon, C. P.; et al. Preclinical Antitumor Activity of a Novel Folate-Targeted Dual Drug Conjugate. *Mol. Pharmaceutics* **2007**, *4* (5), 659–667.

(14) Li, X.; Ding, L.; Xu, Y.; Wang, Y.; Ping, Q. Targeted delivery of doxorubicin using stealth liposomes modified with transferrin. *Int. J. Pharm.* **2009**, *373*, 116–123.

(15) Song, S.; et al. Peptide ligand-mediated liposome distribution and targeting to EGFR expressing tumor in vivo. *Int. J. Pharm.* **2008**, *363* (1−2), 155–161.

(16) Alves, J. B.; et al. Local delivery of EGF-liposome mediated bone modeling in orthodontic tooth movement by increasing RANKL expression. *Life Sci.*, in press.

(17) Yokoe, J.-i. Albumin-conjugated PEG liposome enhances tumor distribution of liposomal doxorubicin in rats. *Int. J. Pharm.* **2008**, *353*, 28–34.

(18) Reubi, J. C.; Kvols, L.; Krenning, E.; Lamberts, S. W. J. Distribution of somatostantin receptors in normal and tumor tissue. *Metabolism* **1990**, *39* (Suppl. 2), 78–81.

(19) Volante, M.; et al. Somatostatin, cortistatin and their receptors in tumours. *Mol. Cell. Endocrinol.* **2008**, *286*, 219–229.

(20) Olsen, J. O.; et al. Somatostatin receptor imaging of neuroendocrine tumors with indium-111 pentetreotide (Octreoscan). *Semin. Nucl. Med.* **1995**, *25* (3), 251–261.

(21) Engel, J. B.; Schally, A. V.; Dietl, J.; Rieger, L.; Hönig, A. Targeted Therapy of Breast and Gynecological Cancers with Cytotoxic Analogues of Peptide Hormones. *Mol. Pharmaceutics* **2007**, *4* (5), 652–658.

(22) Nagy, A.; et al. Synthesis and biological evaluation of cytotoxic analogs of somatostatin containing doxorubicin or its intensely potent derivative, 2-pyrrolinodoxorubicin. *Proc. Natl. Acad. Sci. U.S.A.* **1998**, *95*, 1794–1799.

(23) Kiaris, H.; et al. A targeted cytotoxic somatostatin (SST) analogue, AN-238, inhibits the growth of H-69 small-cell lung carcinoma (SCLC) and H-157 non-SCLC in nude mice. *Eur. J. Cancer* **2001**, *37*, 620–628.

(24) Shen, H.; et al. Paclitaxel-octreotide conjugates in tumor growth inhibition of A549 human non-small cell lung cancer xenografted into nude mice. *Eur. J. Pharmacol.* **2008**, *60* (1−3), 23–29.

(25) Huang, C.-M.; Wu, Y.-T.; Chen, S.-T. Targeting delivery of paclitaxel into tumor cells via somatostatin receptor endocytosis. *Chem. Biol.* **2000**, *7* (7), 453–461.

positive tumor cells and increasing intracellular delivery of antitumor drugs such as DOX. With this hypothesis, we constructed a targeting delivery system of liposomal DOX through combination of passive (PEGylation) and active (Oct modification) delivery strategies. Namely, DOX was encapsulated into Oct modified SSL (Oct-SSL). Three cells with different expression level of SSTR2 were used as model or control. *In vitro* and *in vivo* characteristics of the targeting DDS were investigated in different cell models as well as tumor bearing mice models.

Materials and Methods

Materials. Octreotide acetate (M_w 1019.26) was custom synthesized (purity 98%) by Zaichuang Biotechnology Co., Ltd. (Shanghai, China). DSPE-PEG and DSPE-PEG-NHS (PEG M_w 2000) were purchased from NOF Co. (Tokyo, Japan). Cholesterol and Sephadex G50 were obtained from Pharmacia Biotech (Piscataway, NJ), and EPC was obtained from Lipoid GmbH (Ludwigshafen, Germany). Doxorubicin hydrochloride was kindly provided as a gift by Haizheng Pharmaceutical Co., Ltd. (Zhejiang, China). ICG was purchased from Acros Organics (Geel, Belgium). Trypsin was purchased from AMRESCO Inc. (Solon, OH).

SSTR2 goat polyclonal IgG (sc11606), donkey anti-goat IgG-FITC (sc2024), donkey anti-goat IgG-HRP (sc2020), GAPDH rabbit polyclonal IgG (sc25778) and Western blotting luminol reagent (sc-2048) were sourced from Santa Cruz Biotechnology, Inc. (Santa Cruz, CA). Goat anti-rabbit IgG-HRP was from Zhongshan Golden-Bridge Biotechnology Co., Ltd. (Beijing, China). RIPA lysis buffer (P1053), protease inhibitor (cocktail, P1265), BCA protein assay kits (P1511), 5× SDS−PAGE loading buffer (B1012), X-ray films and cassette were obtained from Applygen Technologies Inc. (Beijing, China). PVDF membrane was obtained from Millipore China (Beijing, China). Prestained protein molecular weight marker (#SM0441) was purchased from Fermentas China (Beijing, China). All other chemicals were of analytical grade purity.

Cell Culture and Animals. Human small cell lung cancer cell line NCI-H446, human breast cancer cell line MCF-7 and Chinese hamster ovary cell line CHO were obtained from Institute of Basic Medical Science, Chinese Academy of Medical Science (Beijing, China). Cells were cultured in RPMI-1640, DMEM and Ham's F12 medium (M&C Gene Technology, Beijing, China) respectively, supplemented with 10% FBS at 37 °C in 5% CO_2 atmosphere.

Male SD rats (180−200 g) and BALB/c nude mice (18−22 g) provided by Vital River Laboratory Animal Center (Beijing, China) were acclimated at 25 °C and 55% humidity under natural light/dark conditions for 3 days before studies, with free access to standard lab food (Vital River Laboratory Animal Center, Beijing, China) and water during experiments. All care and handling of animals were performed with the approval of the Institutional Animal Care and Use Committee at Peking University Health Science Center.

DSPE-PEG−Oct Conjugation. Oct was conjugated to DSPE-PEG through the activated NHS group. DSPE-PEG-NHS was incubated in DMF with Oct at 2:1 molar ratio, adjusting pH to 10.0 with triethylamine. Reaction was performed for 4 days at room temperature under moderate stirring and traced by PR-HPLC (Shimadzu, LC-10AT, Japan). The mobile phase consisted of 30% acetonitrile and 70% PBS (pH 7.4), and UV absorbance was monitored at 220 nm. Finally, the reaction mixture was dialyzed (molecular mass cutoff 3500) against deionized water for 24 h to remove the unconjugated peptide, followed by lyophilization, and stored at −20 °C until used. The structure of DSPE-PEG−Oct was characterized by MALDI-TOF MS. To indicate the coupling site between DSPE-PEG-NHS and Oct, a proteolytic digestion was carried out. Briefly, DSPE-PEG−Oct was treated with dithiothreitol at a final concentration of 5 mM for 4 h to reduce the disulfide bond, followed by treating with trypsin (final concentration 1 mg/mL) in 0.1 M Tris-HCl buffer (pH 8.0) for 1 h at 37 °C.[28−30] The digests were directly analyzed by MALDI-TOF MS. The conjugating sites were identified from the molecular weight of the DSPE-PEG−Oct fragments.

Preparation of Liposomes. Lipid compositions of EPC/cholesterol/DSPE-PEG (15.9:4.1:6.0, w/w) and EPC/cholesterol/DSPE-PEG/DSPE-PEG−Oct (15.9:4.1:5.7:0.3, w/w) were used for SSL-DOX and Oct-SSL-DOX, respectively. Liposomes were prepared by thin lipid film hydration method. Briefly, lipids were dissolved in chloroform in a pear-shaped flask and evaporated at 37 °C on a rotary evaporator until dry. The obtained dried lipid films were hydrated in 123 mM ammonium sulfate, followed by sonication for 10 min. External buffer was exchanged by eluting through a Sephadex G50 column equilibrated with PBS (pH 7.4). DOX was loaded by ammonium sulfate gradient method. In brief, DOX was added into empty liposomes at a lipid−drug ratio of 20:1 (w/w) and incubated for 10 min at 60 °C with gentle shaking. Encapsulated DOX was separated from free DOX through a Sephadex G50 column eluted with PBS (pH 7.4). For liposomes loading

(26) Moody, T. W.; et al. Camptothecin-somatostatin conjugates inhibit the growth of small cell lung cancer cells. *Peptides* **2005**, *26* (9), 1560–1566.

(27) Sun, L.-C.; Luo, J.; Mackey, L. V.; Fuselier, J. A.; Coy, D. H. A conjugate of camptothecin and a somatostatin analog against prostate cancer cell invasion via a possible signaling pathway involving PI3K/Akt, αVβ3/αVβ5 and MMP-2/-9. *Cancer Lett.* **2007**, *246* (1−2), 157–166.

(28) Na, D. H.; et al. Identification of the Modifying Sites of Mono-Pegylated Salmon Calcitonins by Capillary Electrophoresis and MALDI-TOF Mass Spectrometry. *J. Chromatogr., B: Biomed. Sci. Appl.* **2001**, *754* (1), 259–263.

(29) Na, D. H.; Lee, K. C.; DeLuca, P. P. PEGylation of Octreotide: II. Effect of N-terminal Mono-PEGylation on Biological Activity and Pharmacokinetics. *Pharm. Res.* **2005**, *22, 5*, 743–749.

(30) Na, D. H.; DeLuca, P. P. PEGylation of Octreotide_ I. Separation of Positional Isomers and Stability Against Acylation by Poly(D, L-lactide-co-glycolide). *Pharm. Res.* **2005**, *22, 5*, 736–742.

ICG, obtained dried lipid films were hydrated with ICG solution (0.25 mg/mL in water), followed by sonication. All liposomes were stored at 4 °C and used within one week.

Average particle size, PDI and zeta potential of liposomes were determined by dynamic light scattering (DLS) using Malvern Zetasizer Nano ZS (Malvern, U.K.) at 25 °C. Concentration of DOX and ICG was determined by UV spectrophotometry at 485 and 784 nm, respectively.

Drug Release *in Vitro*. To determine the release kinetics of DOX from liposomes, 0.5 mL of liposomes (SSL-DOX or Oct-SSL-DOX) was mixed with 0.5 mL of FBS and placed in a dialysis bag (molecular mass cutoff 3500). Bags were incubated in 50 mL of PBS (pH 7.4) at 37 °C with gentle shaking (100 rpm). Aliquots of 0.5 mL of incubation medium were removed at predetermined time points (0.5, 1, 2, 4, 8, 12, 24, 36, 48 h) and replaced with an equal volume of fresh medium. Released DOX was quantified by fluorophotometer (470/585 nm).

Western Blot Analysis. NCI-H446, MCF-7 and CHO cells were seeded in 6-well plates for one day. Cells were washed with cold PBS three times and then lysed in RIPA buffer for 5 min on ice. Lysate was centrifuged for 10 min at 12000 rpm at 4 °C, and the supernatants were maintained at −20 °C. Protein assay was performed using the BCA method with BSA as standard.

Western blot analysis was carried out by the standard methods. Briefly, samples were solubilized in SDS−PAGE loading buffer for 10 min at 100 °C and resolved on 12% SDS−PAGE gels. Fractionated proteins were then transferred onto PVDF membranes. Membranes were blocked with 5% nonfat milk and incubated with primary antibodies, followed by the corresponding HRP-conjugated secondary antibodies. Signal was visualized by the ECL method using luminol reagent according to the manufacturer's protocol.

Confocal Microscopy Studies. Following the culturing of NCI-H446, MCF-7 and CHO cells for 24 h on 14 mm^2 glass coverslips that were placed in culture dishes, various formulations (free DOX, SSL-DOX or Oct-SSL-DOX) at a DOX concentration of 10 μM were added to each dish and incubated for another 3 h at 37 °C. The medium was removed, and cells were washed with cold PBS followed by fixing with 4% paraformaldehyde in PBS for 10 min. Nuclear staining was performed by Hoechst 33258 for 10 min, and the fluorescent images of cells were analyzed using a laser scanning confocal microscope (LSCM, leica, TCS SP2, Germany).[31]

For SSTR2 expression study, three different cells were cultured on coverslips 24 h prior to experiments. Medium was removed, and cells were washed and fixed, followed by incubation with 100 μL of primary antibody (SSTR2 goat polyclonal IgG, 1:75) overnight at 4 °C. Negative controls (PBS added) were included. Cells were then washed three times with cold PBS and incubated again with 100 μL of secondary antibody (donkey anti-goat IgG-FITC, 1:100) for 1 h at room temperature. Then nuclear staining was conducted and a laser scanning confocal microscope was used as described above.

Fluorescent Detection of Cellular Uptake. To study the kinetics of cellular uptake, NCI-H446 cells (1×10^5 cells per well in a 24-well plate) were incubated with various formulations of DOX-loaded liposomes at 37 °C. The final concentration of DOX was diluted by serum free medium to 10 μM.[32] After incubation, medium was removed and cells were washed with cold PBS three times. An aliquot of 1 mL of DMSO was added to lyse cells. Fluorescence intensity of the DOX in DMSO was determined by fluorophotometer (470/585 nm). Values were then normalized with respect to total cellular protein content, which was quantified by the BCA method. Percentage of uptake was calculated as normalized concentration of uptaked DOX to the concentration of encapsulated DOX being added.[33]

Competition Experiments. Approximately 5×10^5 NCI-H446 cells per well were seeded in a 6-well plate 24 h prior to study, and cells were preincubated with 5 mg/mL excess free Oct or primary antibody (SSTR2 goat polyclonal IgG, 1:75) for 0.5 h at 37 °C to saturate receptors.[34] Then SSL-DOX or Oct-SSL-DOX was added to designated wells with a concentration of DOX as 10 μM. After the incubation period of 3 h, cells were trypsinized and pelleted by centrifugation, then washed three times with cold PBS and examined by flow cytometry using the FACScan (Becton Dickinson, San Jose, CA). Cells associated DOX were excited with an argon laser (488 nm), and fluorescence was detected at 560 nm. Files were analyzed with the FACStation software program.

***In Vitro* Cytotoxicity Study.** Cytotoxicity *in vitro* was assessed in NCI-H446, MCF-7 and CHO cell lines. Cells were plated at a density of 5×10^3 cells per well in 200 μL of medium in 96-well plates and grown for 24 h, and then they were exposed to a series of concentrations of free DOX, SSL-DOX or Oct-SSL-DOX for 6 h, followed by washing with PBS and replacing with fresh medium. Next, cells were additionally incubated for another 42 h (NCI-H446 and MCF-7) or 66 h (CHO). The viability of cells was measured using the MTT method.[35] Briefly, 180 μL of medium with 20 μL of MTT solution (final concentration 0.5 mg/mL) was added to each well and plates were incubated for 4 h at 37 °C. After that, 200 μL of DMSO was added to each well for 10

(31) Tang, N.; et al. Improving Penetration in Tumors With Nanoassemblies of Phospholipids and Doxorubicin. *J. Natl. Cancer Inst.* **2007**, *99*, 13.

(32) Kobayashi, T.; et al. Effect of transferrin receptor-targeted liposomal doxorubicin in P-glycoprotein-mediated drug resistant tumor cells. *Int. J. Pharm.* **2007**, *329*, 94–102.

(33) Hu, F.-Q.; Wu, X.-l.; Du, Y.-Z.; You, J.; Yuan, H. Cellular uptake and cytotoxicity of shell crosslinked stearic acid-grafted chitosan oligosaccharide micelles encapsulating doxorubicin. *Eur. J. Pharm. Biopharm.* **2008**, *69*, 117–125.

(34) Garga, A.; Tisdalea, A. W.; Haidarib, E.; Kokkoli, E. Targeting colon cancer cells using PEGylated liposomes modified with a fibronectin-mimetic peptide. *Int. J. Pharm.* **2009**, *366*, 201–210.

(35) Blumenthal, R. D. *In Vitro Assays*; Humana Press Inc.: Totowa, NJ, 2005; Vol. 1, p 69−78.

min at room temperature. Absorbance was measured at 540 nm using a 96-well plate reader (Biorad, 680, America).

Pharmacokinetic Experiments *in Vivo*. Male SD rats (180−200 g) were randomly divided into 3 groups (6 rats per group) and injected intravenously through the tail vein with free DOX, SSL-DOX or Oct-SSL-DOX (2.5 mg/kg DOX each). At scheduled time points (0.5, 1, 2, 4, 6, 8, 12, 24, 36, 48 h) after injection, blood samples were serially drawn from orbits, and centrifuged for 10 min at 14000 rpm at 4 °C immediately to isolate plasma and stored at −20 °C. Plasma extracts were prepared by mixing plasma with four times volume of methanol. Precipitated proteins were removed by centrifugation for 10 min at 14000 rpm at 4 °C.[36] The clear supernatants were detected by fluorophotometer (470/585 nm). Main PK parameters were calculated by WinNonlin V5.2.

Living Imaging Studies. Approximately 5×10^6 NCI-H446 cells were inoculated subcutaneously in the flank region of nude mice. On the 15th day after tumor inoculation (when the tumor volume reached 1000−1500 mm^3), mice were injected with ICG-loaded SSL or Oct-SSL (5 mg/kg) via the tail vein and then anesthetized using intraperitoneal injection of pentobarbital (60 mg/kg). NIRF imaging experiments were performed at 3, 6, and 9 h postinjection using a Kodak multimodal-imaging system IS2000MM (Kodak, USA) equipped with an excitation bandpass filter at 760 nm and an emission at 830 nm. Exposure time was 60 s per image. Images was analyzed using the imaging station IS2000MM software (Kodak ID Image Analysis Software; Kodak).[37]

After living imaging, mice were sacrificed. Tumors and organs were excised and analyzed again with the same system as described above.

***In Vivo* Antitumor Activity.** Approximately 5×10^6 NCI-H446 cells in 200 μL of serum free medium were subcutaneously incubated into the right flank of mice. When average tumor volume reached about 50 mm^3, mice were randomly assigned to 4 groups ($n = 6$): briefly, group 1 for saline solution as control,[38] group 2 for DOX PBS-solution, group 3 for SSL-DOX and group 4 for Oct-SSL-DOX. Various formulations were intravenously administered with a dose of 2 mg/kg. DOX was given every other day for 5 times, and tumor volumes were measured with a Vernier caliper, and calculated using the following equation:

$$\text{volume } (mm^3) = \text{longer diameter} \times (\text{shorter one})^2 \times 0.5$$

Tumors were also excised from sacrificed mice after 15 days' observation.

Statistical Analysis. All the experiments were repeated at least three times. All data are shown as means ± SD unless particularly outlined. Student's t test or one-way analyses of variance (ANOVA) were performed in statistical evaluation. A value of p less than 0.05 was considered to be significant.

Results and Discussion

DSPE-PEG−Oct Conjugation. The conjugation reaction was monitored by RP-HPLC, and the final product was identified by MALDI-TOF MS as shown in Figure 1. After 4 days, the reaction between peptide and polymer reached equilibrium, with 33.1 ± 3.1% uncoupled Oct. As Oct has two functional amino groups (at the N-terminus and the side chain of Lys), both reactive, we may get mono- or disubstituted derivatives (Figure 1A). But in our test condition, the appearance of peaks in the *m/z* range around 4000 and no peak around 5000 in the MALDI-TOF MS (Figure 1D,E) indicated that DSPE-PEG and Oct conjugated at a molar ratio of 1:1. In order to further confirm the coupling site, a Lys-C digestion test was performed. Trypsin cleaves peptide chains mainly at the carboxyl side of lysine or arginine, except when either is followed by proline. Oct has only one Lys residue. If PEGylation occurred at the Lys residue, there would be no change in the mass spectrum after trypsinization; otherwise the modification occurring at the N-terminus would exhibit a reduced mass fragment.[30] As shown in Figure 1F, DSPE-PEG−Oct digests produced mass peaks around *m/z* 3700. These results indicated that the conjugation occurred at the N-terminus of Oct.

Liposome Preparation. All liposomes prepared were ~100 nm (PDI < 0.30) with negative charge on the surface. The loading efficiency of DOX was consistently greater than 95% (Table 1). The concentration of DOX was about 300 μg/mL, and the amount of lipid (liposomes) was about 6 mg/mL. Stored at 4 °C, no significant leakage of DOX was found within one week. All these parameters were not significantly affected by the Oct modification.

***In Vitro* Release of DOX.** The profiles of DOX release versus time *in vitro* are presented in Figure 2. To better simulate conditions *in vivo*, we preferred to mix liposomes with FBS directly. After 48 h about 40% of DOX released from liposomes, suggesting a favorable drug releasing property at this condition. The relatively slow leakage of DOX from lipid vesicles was likely due to its encapsulation mechanism. However, there were no significant differences between SSL-DOX and Oct-SSL-DOX in drug release at each time point, indicating little effect by the peptide modification.

Expression Level of SSTR2 in Different Cell Lines. Obviously, the receptor-mediated endocytosis is very much dependent on the expressing level of receptors. It was reported that Oct showed high affinity to SSTRs, especially

(36) Fundaro, A.; et al. Nonstealth and stealth solid lipid nanoparticles SLN carrying doxorubicin pharmacokinetics and tissue distribution after iv administration to rats. *Pharmacol. Res.* **2000**, *42* (4), 337–343.

(37) Peng, L.; et al. Combinatorial chemistry identifies high-affinity peptidomimetics against a4b1 integrin for in vivo tumor imaging. *Nat. Chem. Biol.* **2006**, *2*, 7.

(38) Ogawara, K.-i.; Un, K.; Tanaka, K.-i.; Higaki, K.; Kimura, T. In vivo anti-tumor effect of PEG liposomal doxorubicin (DOX) in DOX-resistant tumor-bearing mice: Involvement of cytotoxic effect on vascular endothelial cells. *J. Controlled Release* **2009**, *133*, 4–10.

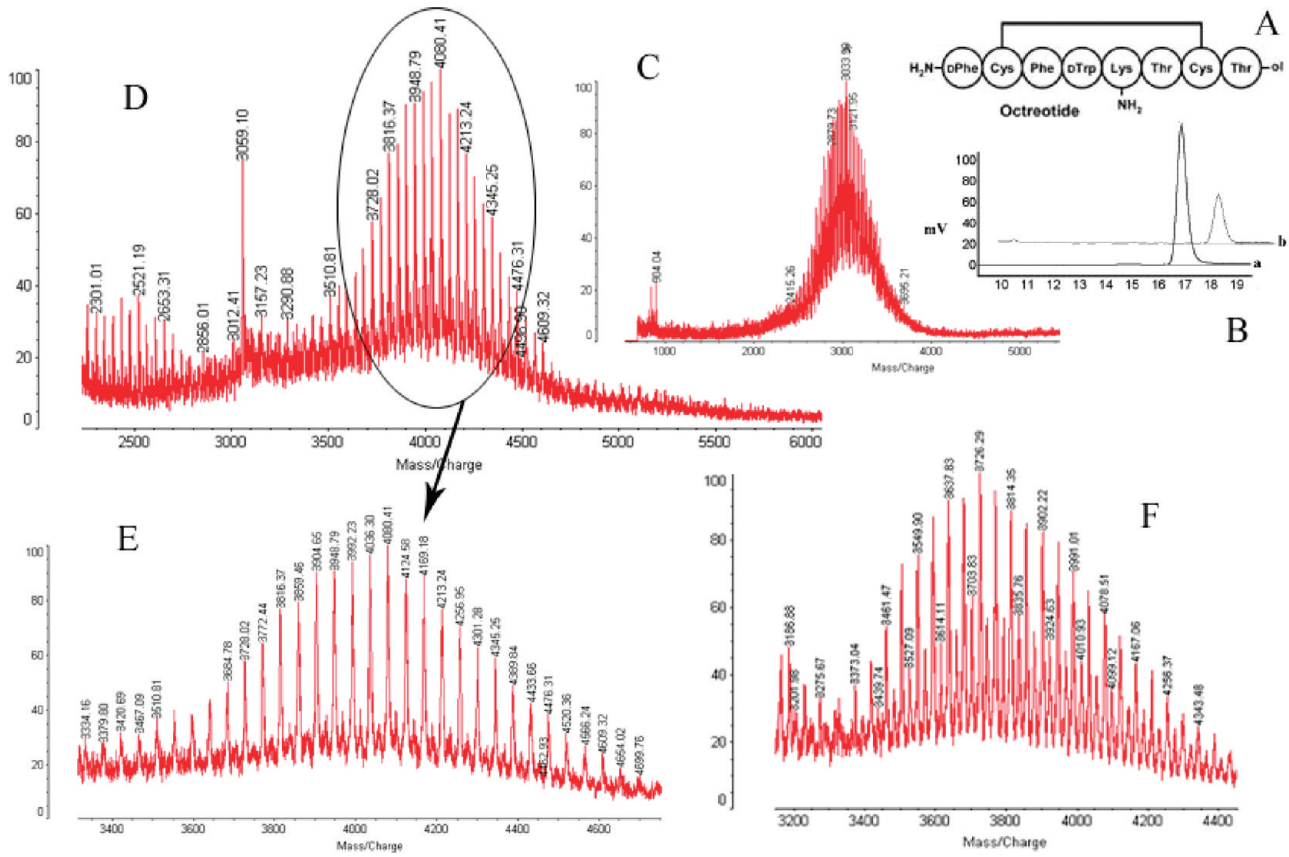

Figure 1. Conjugation of Oct to DSPE-PEG-NHS. (A) Amino acid sequence of Oct which has two amino groups (at the N-terminus and the side chain of Lys). (B) HPLC determination of unconjugated peptide: (a) free Oct in mobile phase and (b) DSPE-PEG-NHS and Oct with a molar ratio of 2:1 in mobile phase after reaction for 4 days. (C) Mass spectrum of DSPE-PEG-NHS with a peak at the *m*/*z* range around 3000. (D, E) Mass spectrum of DSPE-PEG−Oct with a peak at the *m*/*z* range around 4000 and there was no peak around 5000. (F) Mass spectrum of DSPE-PEG−Oct digested by trypsin with a peak at the *m*/*z* range around 3700. MALDI-TOF MS results indicated that DSPE-PEG-NHS and Oct conjugated at the N-terminus of Oct with a molar ratio of 1:1.

Table 1. Characteristics of Different Formulations of Sterically Stabilized Liposomes ($n = 3$)

formulation	size (nm)	PDI	zeta potential (mV)	encapsulation efficiency (%) of DOX
SSL	86.03 ± 0.88	0.23 ± 0.03	−4.86 ± 1.17	
SSL-DOX	92.02 ± 2.68	0.22 ± 0.03	−5.27 ± 1.29	97.3 ± 2.03
Oct-SSL	87.56 ± 2.93	0.23 ± 0.03	−4.97 ± 1.24	
Oct-SSL-DOX	93.95 ± 1.55	0.24 ± 0.01	−4.70 ± 0.89	96.3 ± 1.08

subtype 2,[39] and both NCI-H446 and MCF-7 cell lines expressed SSTR2.[40,41] Therefore, it is necessary to detect the expression level of SSTR2 on these kinds of cancer cell lines. The CHO cell line was used as negative control.[25] The

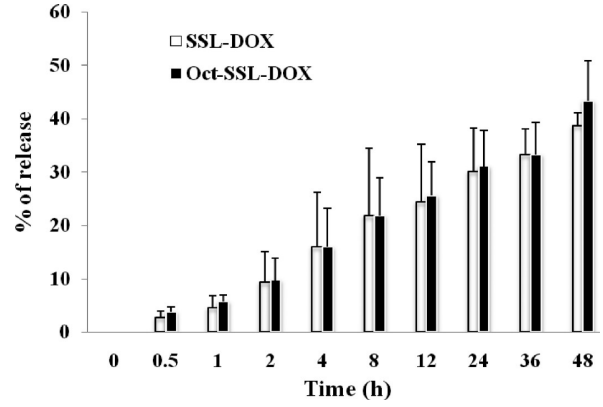

Figure 2. *In vitro* release of DOX from liposomes. 0.5 mL of liposomes and 0.5 mL of FBS were mixed in a dialysis bag (molecular mass cutoff 3500) and incubated at 37 °C in 50 mL of PBS. At predetermined time points, 0.5 mL of medium was replaced, and the amount of DOX was quantified as described in Materials and Methods ($n = 3$).

results (Figure 3) showed obvious expression of SSTR2 on the surface of NCI-H446 and MCF-7, while there was no SSTR2 detected on CHO. Furthermore, NCI-H446 exhibited

(39) Siehler, S.; Seuwen, K.; Hoyer, D. [^{125}I][Tyr^3]octreotide labels human somatostatin sst2 and sst5 receptors. *Eur. J. Pharmacol.* **1998**, *348*, 2–3.
(40) Xu, B.; et al. Expression of somatostatin receptor subtype 2 in 12 tumor cell lines. *Guangdong Med. J.* **2006**, *27*, 3.
(41) Watt, H. L.; Kumar, U. Colocalization of somatostatin receptors and epidermal growth factor receptors in breast cancer cells. *Cancer Cell Int.* **2006**, *6*, 5–23.

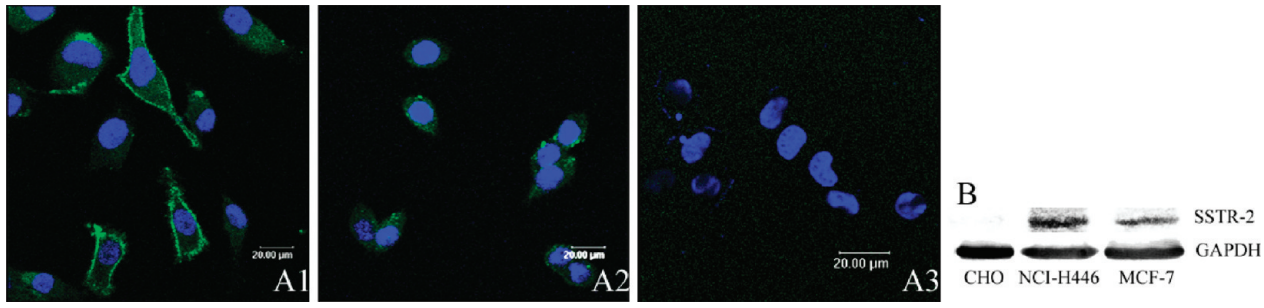

Figure 3. Expression level of SSTR2 in different cell lines. (A) Confocal microscopy images of SSTR2-expressing detection on NCI-H446 (A1), MCF-7 (A2) and CHO (A3) cell lines. Green represents fluorescence of FITC (secondary antibody conjugated). Blue represents fluorescence of Hoechst 33258. (B) Western blot analysis of SSTR2 expression level in three cell lines. Cell lysates were separated by 12% SDS−PAGE gels and blotted with anti-SSTR2 (41 kDa) antibody; GAPDH (37 kDa) was used as loading control. Obviously, receptors expressed on the NCI-H446 cell line were more than those on the MCF-7 cell line, and it was hardly detectable on the CHO cell line.

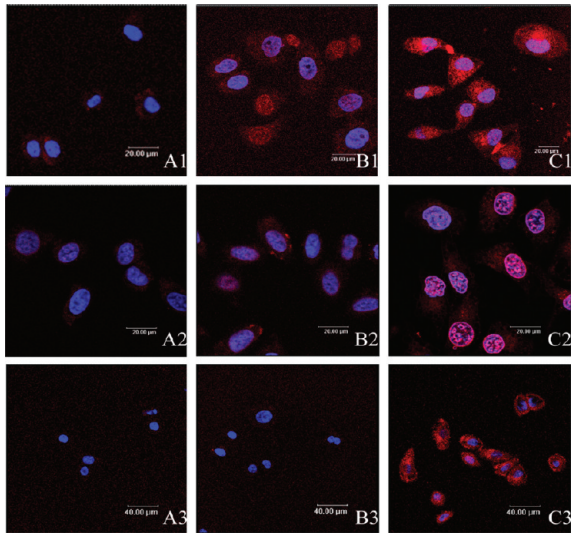

Figure 4. Confocal microscopy images of NCI-H446 (1), MCF-7 (2) and CHO (3) cells incubated with SSL-DOX (A), Oct-SSL-DOX (B) or free DOX (C) for 3 h at 37 °C. The concentration of DOX was 10 μM for all formulations. Red represents fluorescence of DOX. Blue represents fluorescence of Hoechst 33258.

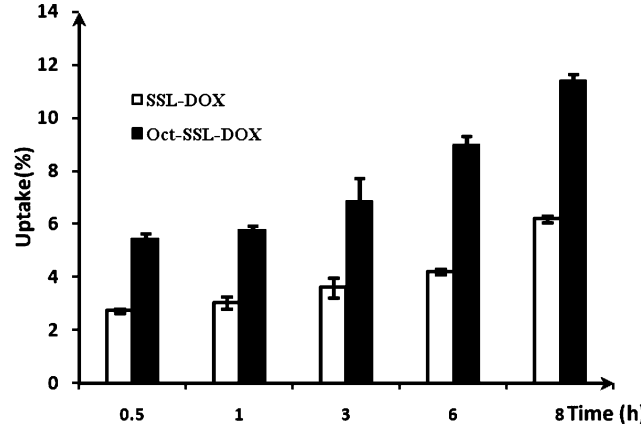

Figure 5. The uptake percentage of SSL-DOX and Oct-SSL-DOX by NCI-H446 cells. Cells were incubated with various formulations (10 μM DOX equivalent) at 37 °C. Each column represents average uptake (%) ± SD ($n = 3$).

more than MCF-7. Therefore, the NCI-H446 cell line was preferred throughout the whole study unless particularly outlined.

Confocal Microscopy Studies. Figure 4 showed the confocal microscopy images of NCI-H446, MCF-7 and CHO cells after 3 h incubation with SSL-DOX, Oct-SSL-DOX or free DOX at 37 °C. Without the release process, free DOX directly penetrated into cells through the membrane diffusion, leading to a greater amount of intracellular accumulation, which was taken as positive control (C1, C2 and C3). For NCI-H446, the images of the Oct-SSL-DOX group (B1) displayed more red fluorescence of DOX than that of the SSL-DOX one (A1), suggesting the favorable effect of Oct on the cellular uptake of liposomes. A similar result was observed on MCF-7 (A2, B2), while the difference between the two liposomal groups was minor compared with NCI-H446, likely due to their difference in SSTR2 expression level. In terms of CHO (A3, B3), there was no red fluorescence in both passive and active targeting liposome groups, proving no expression of SSTR2 on the cells and no targeting effect of Oct to this cell line.

Cellular Uptake Studies on NCI-H446 Cells. The kinetic uptake of SSL-DOX and Oct-SSL-DOX by NCI-H446 cells at 37 °C was shown in Figure 5. It could be seen that both SSL-DOX and Oct-SSL-DOX demonstrated increasing cellular uptake of DOX with the extension of incubation time. Meanwhile, Oct-SSL-DOX exhibited 2.0-, 1.9-, 1.9-, 2.1-, and 1.8-fold cellular uptake over that of SSL-DOX after cultured at 37 °C for 0.5, 1, 3, 6, and 8 h, respectively. It was indicated that Oct facilitated the uptake of liposomal DOX by cancer cells overexpressing SSTR2.

Competition Inhibition Studies. As shown in Figure 6, both primary antibody (anti-SSTR2) and excess free Oct (5 mg/mL) significantly inhibited the uptake of Oct-SSL-DOX by NCI-H446 cells at 37 °C. The preoccupation of receptors led to decreased fluorescence intensity of DOX in cells. Results here demonstrated that the process of cellular uptake of Oct-SSL-DOX was mediated by a mechanism of ligand−receptor interaction, especially the Oct−SSTR2 interaction.

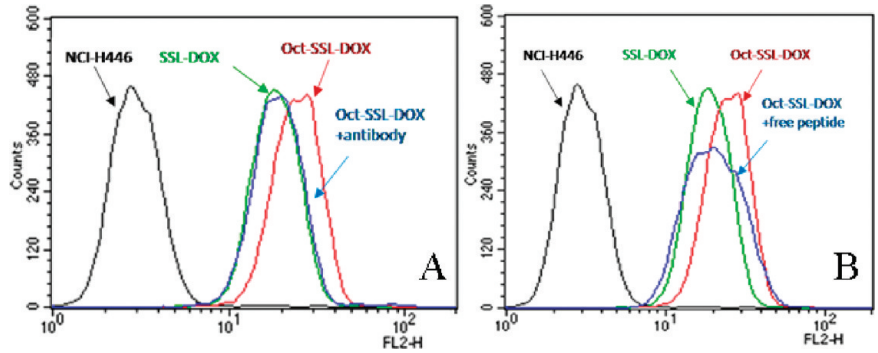

Figure 6. Competition experiments. NCI-H446 cells were pretreated with anti-SSTR2 primary antibody (A) or excess free Oct at 5 mg/mL (B) for 0.5 h at 37 °C followed by incubation with SSL-DOX or Oct-SSL-DOX for 3 h. Flow cytometric curves were obtained. Enhanced cellular uptake by Oct modification was completely blocked in the presence of primary antibody or free peptide.

Table 2. Cytotoxicity of Free DOX, SSL-DOX and Oct-SSL-DOX in NCI-H446, MCF-7 and CHO Cells[a]

	IC50 (μM)		
	free DOX	SSL-DOX	Oct-SSL-DOX[b]
NCI-H446	3.41 ± 0.31	14.7 ± 1.9†	5.63 ± 0.99†,*
MCF-7	1.61 ± 0.52	5.04 ± 1.1†	2.44 ± 0.71†,*
CHO	0.0873 ± 0.022	0.220 ± 0.055†	0.230 ± 0.053†

[a] Cytotoxicity was determined using the MTT assay as described in Materials and Methods. IC50 is the half-maximal inhibitory concentration. Values are expressed as the mean ± SD (n = 3). [b] *p < 0.05 vs SSL-DOX group; †p < 0.05 vs free DOX group.

It was easy to notice that the result from every cellular uptake test with NCI-H446 cells was consistent, and the uptake in different cells was in agreement with their expression level of SSTR2. Additionally, all the cellular uptake studies actually proved in another way that Oct was functionally conjugated on the surface of liposomes and its activity retained.

Cytotoxicity. Free DOX, SSL-DOX and Oct-SSL-DOX were compared in MTT assay in three cell lines (Table 2). To minimize nonspecific adsorption of liposomes to cells and reduce the impact of released DOX from liposomes,[42] we exposed cells to drugs for only 6 h. In order to renew the state of cells after removing drugs, cells were incubated for another 42 h (NCI-H446 and MCF-7) or 66 h (CHO) according to their quantity. It was found that the IC50 of Oct-SSL-DOX was lower than that of SSL-DOX in two SSTR2 positive cell lines, and the gap in NCI-H446 was about 2.6-fold, larger than that in MCF-7 (about 2.0-fold). There is no significant difference between SSL-DOX and Oct-SSL-DOX in CHO. These results also agreed with the expression level of SSTR2 in different cells. It was also observed that the IC50 value for CHO was lowest in each drug group, and the value for MCF-7 was lower than that for NCI-H446. Although the reason is not clear, the cytotoxicity *in vitro* might be an integrated result of drug, drug release from liposomes, modification on the surface of liposomes, the type, characteristics and state of cells, and so on.

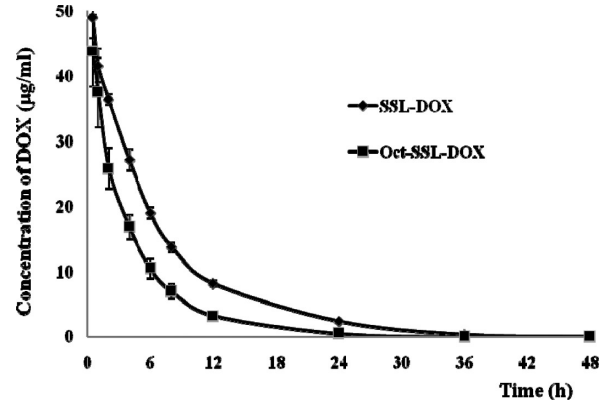

Figure 7. Plasma DOX concentration−time profiles following iv administration of free DOX, SSL-DOX (◆) or Oct-SSL-DOX (■) at a dose of 2.5 mg/kg as DOX to male SD rats. Concentrations of DOX in free DOX group could not be detected even at the first sampling interval (0.5 h). Both liposomes prolonged the circulation time of DOX in rats, while Oct-SSL-DOX showed faster clearance than SSL-DOX.

Pharmacokinetic Character. The plasma concentrations of DOX in free DOX group were too low to detect even at half an hour, while it was detectable in liposomal groups 48 h after intravenous administrations (Figure 7). As anticipated, both SSL-DOX and Oct-SSL-DOX could prolong circulation time of DOX in rats. Besides, the calculated AUC of SSL-DOX in plasma was larger than that of Oct-SSL-DOX, while the apparent distribution volume and clearance of Oct-SSL-DOX were greater or faster than that of SSL-DOX (Table 3), respectively. It was suggested from this study that the long-circulation effect of SSL was maintained but somehow affected after the modification of Oct.

Tissue Distribution Assay *in Vivo* with NIRF Imaging. To evaluate the targeting effect of Oct modified liposome and its tissue distribution *in vivo*, we prepared liposomes loading ICG, which is a water-soluble fluores-

(42) Ahmad, I.; Allen, T. M. Antibody-mediated Specific Binding and Cytotoxicity of Liposome-entrapped Doxorubicin to Lung Cancer Cells in Vitro. *Cancer Res.* **1992**, *52*, 4817–4820.

Table 3. Main Pharmacokinetic Parameters in Plasma after Intravenous Administration of SSL-DOX or Oct-SSL-DOX to Rats[a]

formulation	AUC ((μg/mL)h)	*k* (1/h)	$T_{1/2}$ (h)	V_d (mL)	Cl (mL/h)
SSL-DOX	384 ± 13	0.11 ± 0.016	6.3 ± 0.96	8.30 ± 1.5	0.91 ± 0.032
Oct-SSL-DOX	219 ± 34**	0.15 ± 0.010*	4.7 ± 0.31**	11.4 ± 3.5**	1.7 ± 0.56**

[a] Each preparation was dosed at 2.5 mg/kg as DOX. AUC, area under the plasma concentration−time curve; *k*, elimination rate constant; $T_{1/2}$, plasma half-life; V_d, apparent distribution volume; and Cl, clearance, were calculated based on one-compartment model. Results are expressed as the mean ± SD. *$p < 0.01$ and **$p < 0.05$ vs SSL-DOX group.

cence dye with EX 795 nm and EM 835 nm (DOX was not considered as optional dye here for its EX 488 nm was not suitable for NIRF imaging). And the ICG liposomes were first tested here in the NIRF imaging study. The use of ICG as fluorescence dye but not lipid-soluble ones like Cy5 series is based on the existence of Oct. Activated lipid-soluble dyes could label liposomes via covalent bond with activated NH_2 group of DSPE-PEG, but such a group also exists in the active site of Oct. Therefore, water-soluble dyes like ICG were preferred, which was commonly used clinically in angiography, and reported as label reagent in inhalant powder[43] and nanoparticles.[44,45] The ICG liposomes prepared here were 100−110 nm and negatively charged on the surface with a loading efficiency of ICG greater than 95%.

During the living imaging test, the fluorescence signals in whole bodies of mice were relatively weak (data not show). However, further experiment with excised organs (Figure 8) clearly demonstrated that most of the ICG accumulated in liver 3 h after iv administration of various ICG formulations. Both liposomal formulations increased the fluorescence in liver, spleen, kidneys and lung, and the strongest fluorescence was found in the SSL-ICG group. Similar results can be seen in Figure 8B. Considering the liver-specific distribution of ICG itself and RES uptake of particulates in circulation, these data seemed reasonable and were in accordance with the pharmacokinetics assay.

For the tumor accumulation, it was found that active targeting liposomes enhanced the ICG distribution in tumor compared to passive vesicles as shown in Figure 8A, although the signal in tumor was relatively weak. More clear images could be seen in Figure 8C. The ICG fluorescence in the Oct-SSL-ICG group was the strongest even 9 h after dosing, stronger than that of SSL-ICG at each time point, while there was already no signal detected

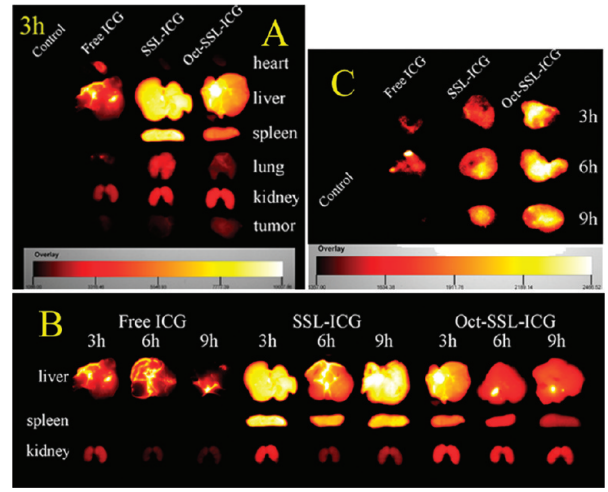

Figure 8. NIRF imaging of main organs at 3 h (A) after iv injection of ICG formulations; and at various time points (B), including excised tumors. (C) The color on images represents fluorescence from ICG.

at 9 h in the free ICG group. In this way, it was proved *in vivo* that Oct-SSL enhanced targeting delivery of DOX to related tumor tissue.

Antitumor Effect *in Vivo*. Figure 9 shows the PD of various DOX formulations on nude mice bearing NCI-H446 cancer xenografts. It was demonstrated that the tumor growth inhibition efficacy of Oct-SSL-DOX was better than that of SSL-DOX ($P < 0.05$). The strongest antitumor effect of Oct-SSL-DOX revealed its highest targeting efficiency. Free DOX showed nearly the same efficacy with the SSL-DOX group, similar to the previous reports,[3] suggesting no correlation between PK and PD, and also the necessity of active targeting. Besides, it was indicated that the antitumor efficacy *in vivo* for Oct-SSL-DOX and SSL-DOX was consistent with the drug distribution in tumor and cell experiments *in vitro*.

Conclusions

A novel DOX-loaded and Oct-modified SSL was prepared and studied here. Various investigations in cell level achieved similar results, namely, the active SSL exhibited higher cell uptake than that of passive SSL in SSTR2-positive cells. The mechanism was proved to be SSTR2 mediated endocytosis. Besides, the Oct modification on the SSL showed little impact on the *in vitro* properties of SSL, however it reduced the circulation time of loaded-DOX to some extent in rats, increased cytotoxicity in SSTR2-positive tumor cells, en-

(43) Mizuno, T.; Mohri, K.; Nasu, S.; Danjo, K.; Okamoto, H. Dual imaging of pulmonary delivery and gene expression of dry powder inhalant by fluorescence and bioluminescence. *J. Controlled Release* **2009**, *134*, 149–154.

(44) Kirchherr, A.-K.; Briel, A.; Mäder, K. Stabilization of Indocyanine Green by Encapsulation within Micellar Systems. *Mol. Pharmaceutics* **2009**, *6, 2*, 480–491.

(45) Ohashi, K.; Kabasawa, T.; Ozeki, T.; Okada, H. One-step preparation of rifampicin/poly(lactic-co-glycolic acid) nanoparticle-containing mannitol microspheres using a four-fluid nozzle spray drier for inhalation therapy of tuberculosis. *J. Controlled Release* **2009**, *135*, 19–24.

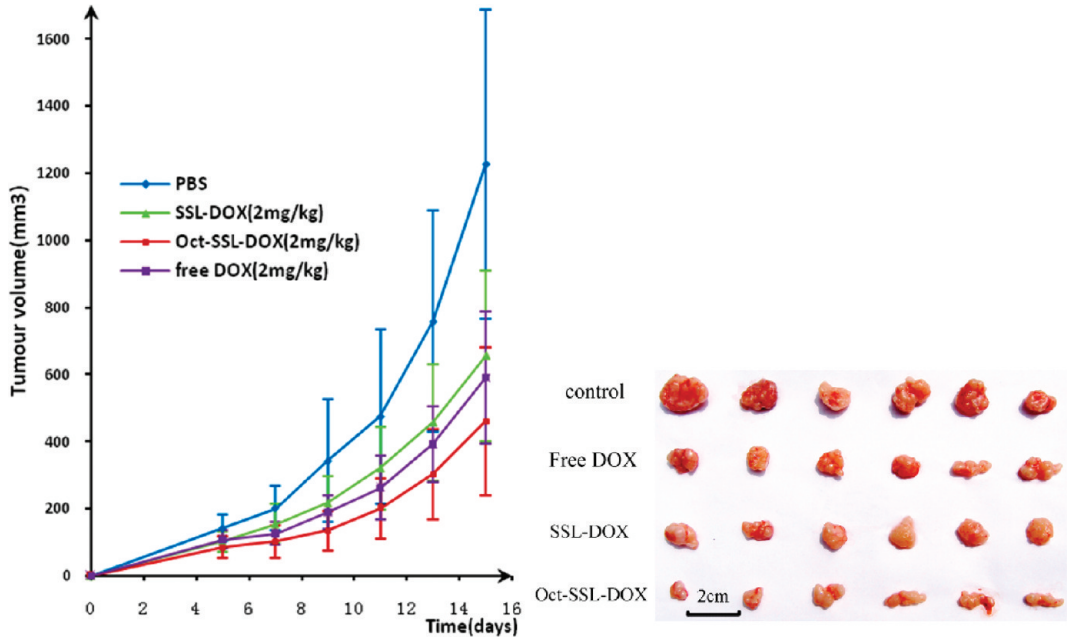

Figure 9. Antitumor activity in NCI-H446-bearing nude mice treated by different DOX formulations. Data represent mean ± SD ($n = 6$). Tumors were excised at the end of the tests.

hanced drug accumulation in tumor tissue and improved anticancer efficacy in SSTR2-overexpressing tumor model, compared to SSL. A correlation was found among intracellular uptake, cytotoxicity, drug distribution in tumor and pharmacodynamic effect of Oct-SSL-DOX in the test conditions. Based on the above observations, we conclude that octreotide-modified SSL may represent a potential strategy for the treatment of SSTR2-overexpressing cancers by enhancing the intracellular uptake of the entrapped anticancer drugs.

Abbreviations Used

Oct, octreotide; DOX, doxorubicin; SSL, sterically stabilized liposomes; SSL-DOX, DOX-loaded sterically stealth lipsosomes; Oct-SSL-DOX, DOX-loaded and Oct-modified sterically stabilized liposomes; SST, somatostatin; SSTRs, somatostatin receptors; SSTR2, somatostatin receptor subtype 2; EPC, egg phosphatidylcholine; PBS, phosphate-buffered saline; DSPE-PEG (PEG M_w 2000), 1,2-distearoyl-*sn*-glycero-3-phosphoethanolamine-*N*-[poly(ethylene-glycol)]; DSPE-PEG-NHS (PEG M_w 2000), 1,2-distearoyl-*sn*-glycero-3-phosphoethanolamine-*N*-[poly(ethylene-glycol)]-*N*-hydroxysuccinimide; DSPE-PEG−Oct, conjugate that Oct covalently linked to DSPE-PEG; SDS−PAGE, sodium dodecyl sulfate polyacrylamide gel electrophoresis; HRP, horseradish peroxidase; MTT, 3-[4,5-dimethylthiazol-2-yl]-2,5-diphenltetrazolium bromide; IC50, 50% inhibitory concentration; AUC, area under concentration−time curves; FBS, fetal bovine serum; PDI, polydispersity index; ICG, indocyanine green; NIRF, near-infrared fluorescence; MOL-TOF MS, matrix-assisted laser desorption/ionization time-of-flight mass spectrometry; PK, pharmacokinetics; PD, pharmacodynamics; BCA, bicinchoninic acid; BSA, bovine serum albumin; ECL, enhanced chemiluminescence; RES, reticulo-endothelial system; DDS, drug delivery system; EGF, epidermal growth factor; DMF, dimethyl formamidine; DMSO, dimethyl sulfoxide.

Acknowledgment. This study was supported by the National Basic Research Program of China (No. 2009CB930300), State Key Projects (No. 2009ZX09310-001) and the 863 Project (No. 2007AA021811). We would like to acknowledge Vivian D. W. Chow for her correction on English writing of this paper.

MP1000235